Electronic supplementary information (ESI)

Complex Isomerism Influencing the Texture Properties of Organometallic [Cu(salen)] Porous Polymers: Paramagnetic Solid-State NMR Characterization and Heterogeneous Catalysis

David Šorm[a]*, Jan Blahut[b]*, Bogdana Bashta[a], Ivana Císařová[c], Eva Vrbková[d], Eliška Vyskočilová[d] and Jan Sedláček[a]

[a] Department of Physical and Macromolecular Chemistry, Faculty of Science, Charles University, Hlavova 2030, Prague 2, 128 43, Czech Republic

[b] Institute of Organic Chemistry and Biochemistry of the Czech Academy of Sciences, Flemingovo náměstí 542/2, Prague 6, 160 00, Czech Republic

[c] Department of Inorganic Chemistry, Faculty of Science, Charles University, Hlavova 2030, Prague 2, 128 43, Czech Republic

[d] Department of Organic Technology, University of Chemistry and Technology Prague, Technická 5, Prague 6, 166 28, Czech Republic

*corresponding authors

L1:
(1*S*,2*S*)-*N,N'-bis*(5-ethynylsalicylidene)-1,2-diaminocyclohexane

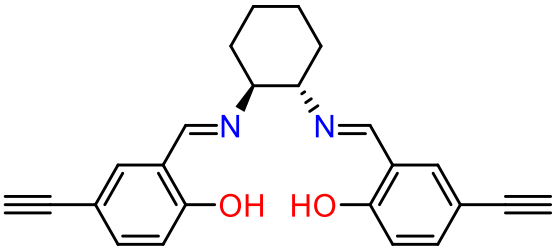

Figure S1: Structure of the ligand **L1**

^{1}H NMR (400 MHz, CD_2Cl_2) δ 13.52 (s, 2H), 8.25 (s, 2H), 7.37 (d, *J* = 2.1 Hz, 2H), 7.34 (s, 2H), 6.82 (d, *J* = 8.7 Hz, 2H), 3.38 – 3.29 (m, 2H), 3.00 (s, 2H), 2.00 – 1.81 (m, 2H), 1.79 – 1.65 (m, 2H), 1.57 – 1.43 (m, 4H).

^{13}C NMR (101 MHz, CD_2Cl_2) δ 164.36, 162.08, 136.13, 135.73, 118.95, 117.57, 112.46, 83.27, 75.88, 72.86, 33.30, 24.52.

HR-MS ESI, measured (calculated) m/z of M+H adduct: 371.174411 (371.175404), $C_{24}H_{23}N_2O_2$

L2:
trans-N,N'-bis(5-ethynylsalicylidene)-1,2-diaminocyclohexane

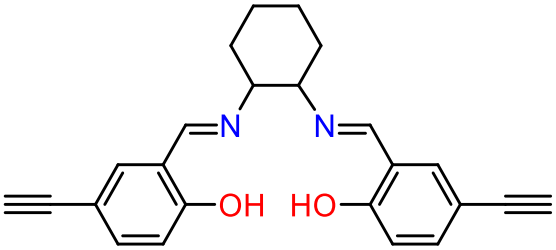

Figure S2: Structure of the ligand **L2**

^{1}H NMR (400 MHz, CD_2Cl_2) δ 13.52 (s, 2H), 8.25 (s, 2H), 7.37 (d, *J* = 2.1 Hz, 2H), 7.34 (s, 2H), 6.82 (d, *J* = 8.8 Hz, 2H), 3.40 – 3.33 (m, 2H), 3.00 (s, 2H), 1.98 – 1.85 (m, 2H), 1.79 – 1.65 (m, 2H), 1.56 – 1.44 (m, 4H).

^{13}C NMR (101 MHz, CD_2Cl_2) δ 164.36, 162.08, 136.13, 135.73, 118.95, 117.57, 112.46, 83.27, 75.88, 72.85, 33.30, 24.52.

HR-MS ESI, measured (calculated) m/z of M+H adduct: 371.174846 (371.175404), $C_{24}H_{23}N_2O_2$

L3:
cis-N,N'-bis(5-ethynylsalicylidene)-1,2-diaminocyclohexane

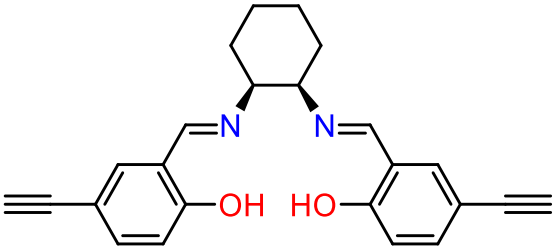

Figure S3: Structure of the ligand **L3**

^{1}H NMR (400 MHz, CD_2Cl_2) δ 13.76 (s, 2H), 8.33 (s, 2H), 7.46 – 7.37 (m, 4H), 6.86 (d, *J* = 8.4 Hz, 2H), 3.66 – 3.58 (m, 2H), 3.03 (s, 2H), 2.02 – 1.73 (m, 4H), 1.67 – 1.51 (m, 4H).

^{13}C NMR (101 MHz, CD_2Cl_2) δ 164.00, 162.40, 136.23, 135.74, 119.10, 117.77, 112.37, 83.38, 75.88, 69.76, 31.10, 22.74.

HR-MS ESI, measured (calculated) m/z of M+H adduct: 371.174930 (371.175404), $C_{24}H_{23}N_2O_2$

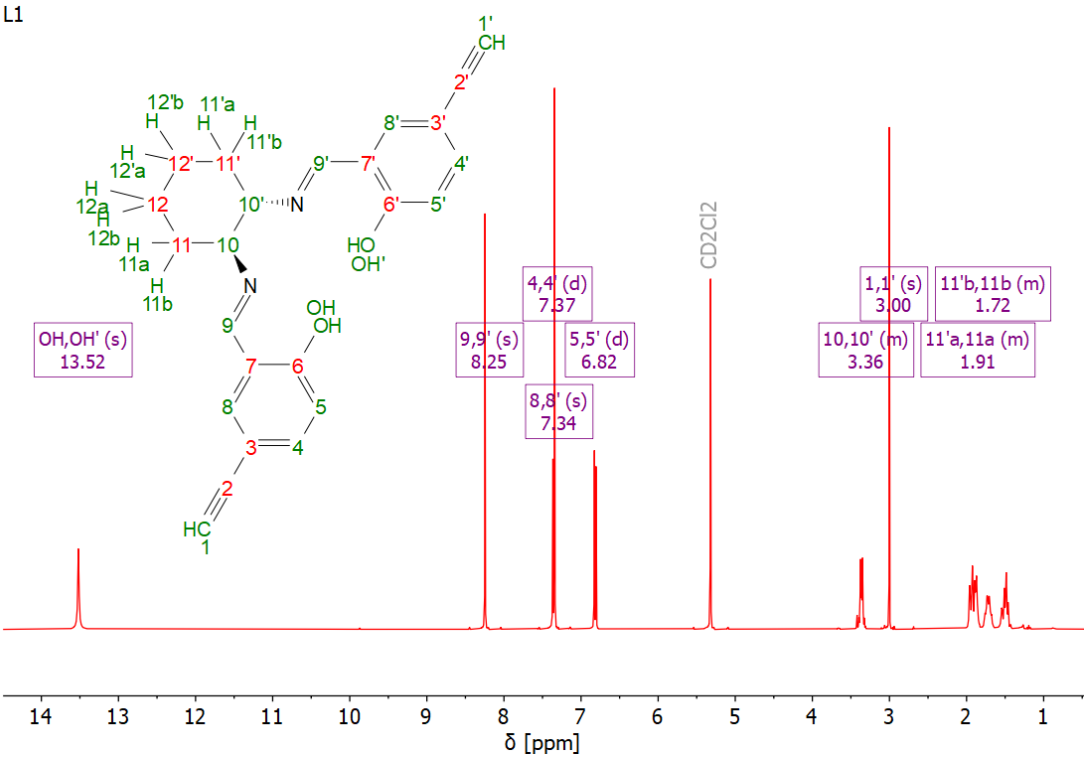

Figure S4: ^{1}H NMR spectrum of **L1** ligand

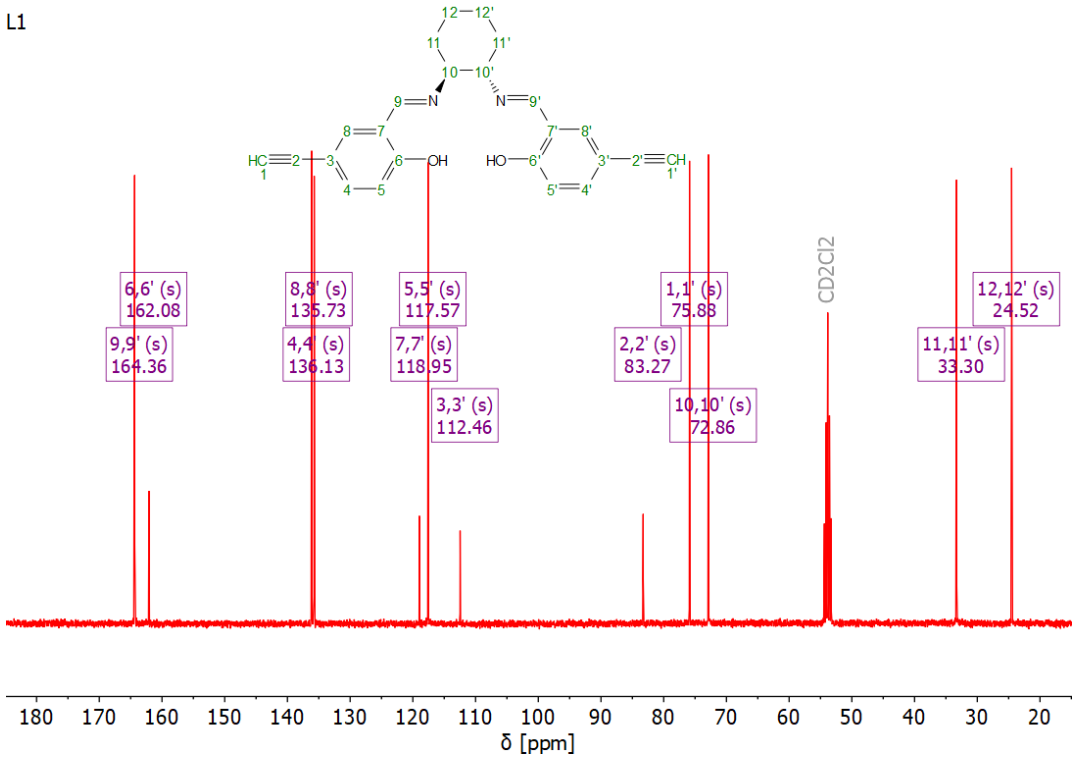

Figure S5: ^{13}C{^{1}H} NMR spectrum of **L1** ligand

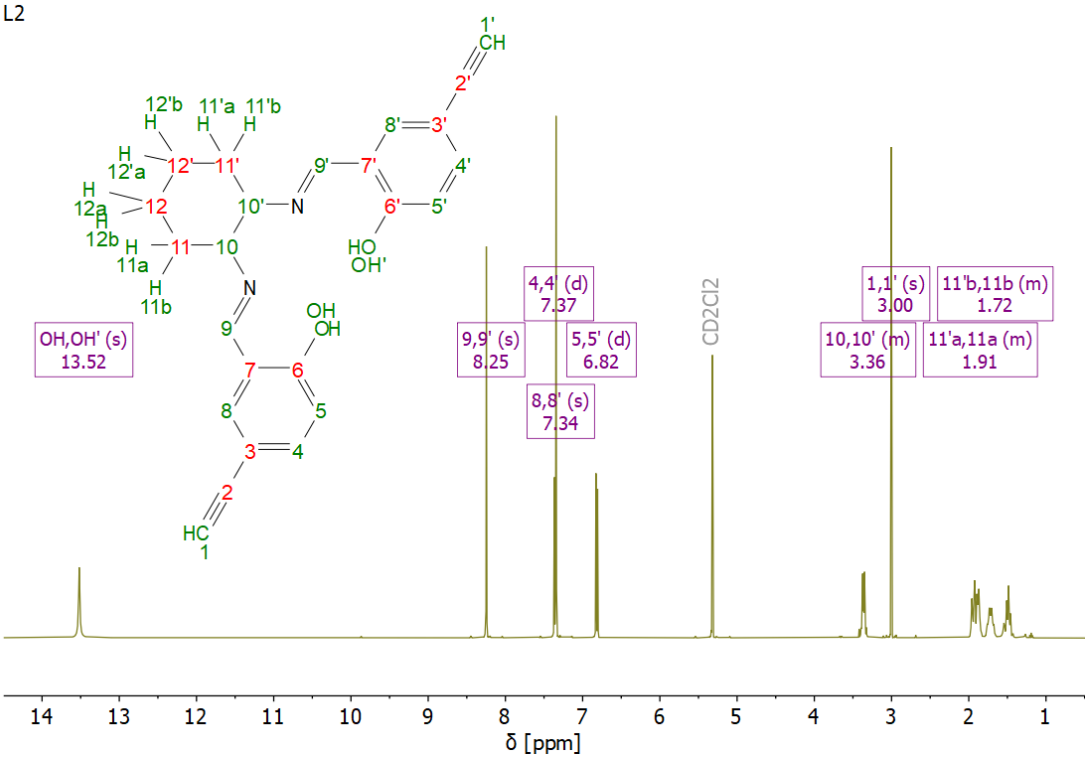

Figure S6: ^{1}H NMR spectrum of **L2** ligand

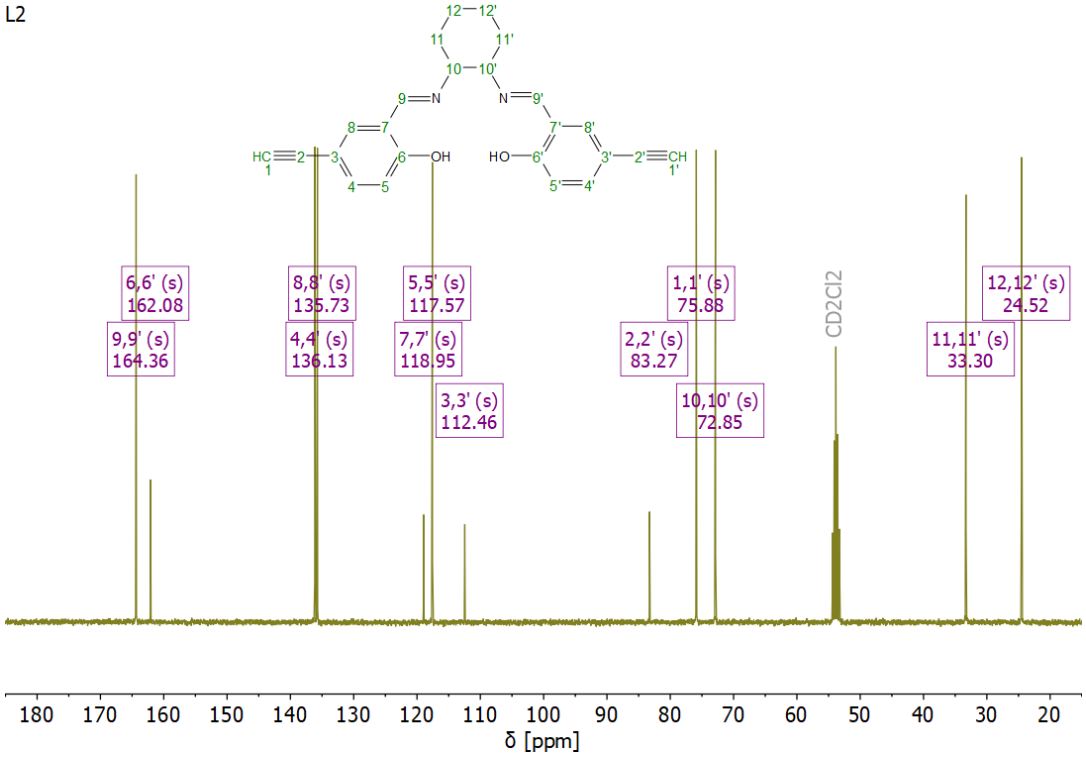

Figure S7: ^{13}C{^{1}H} NMR spectrum of **L2** ligand

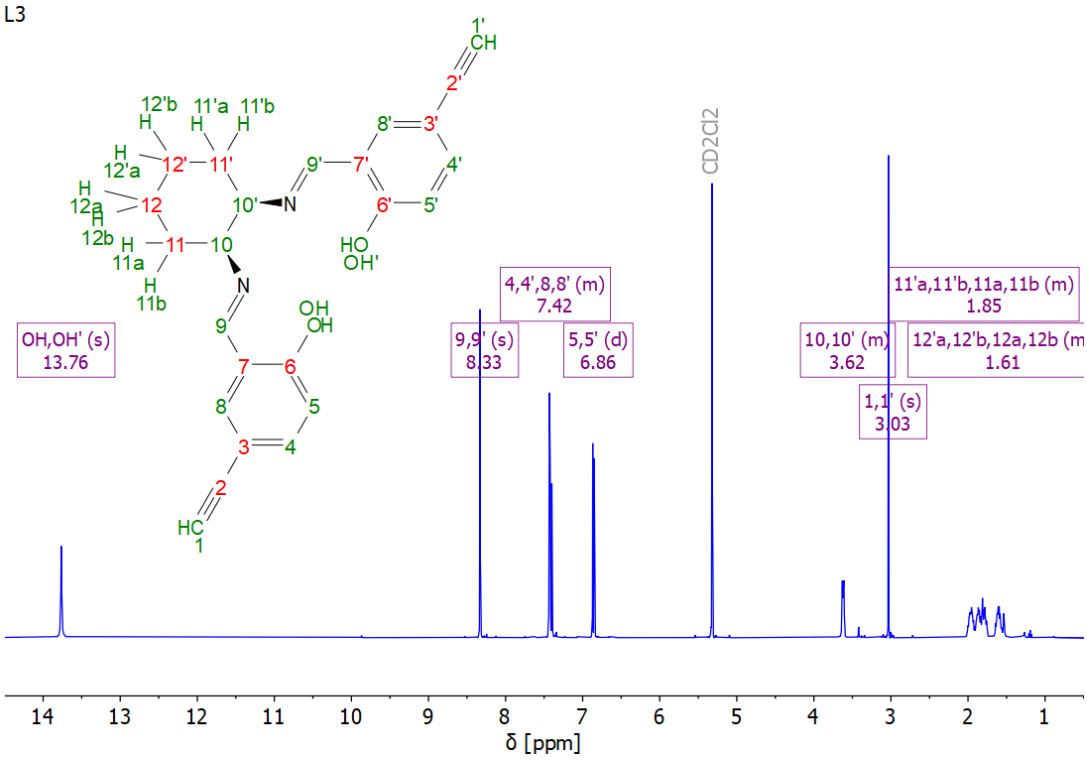

Figure S8: ^{1}H NMR spectrum of **L3** ligand

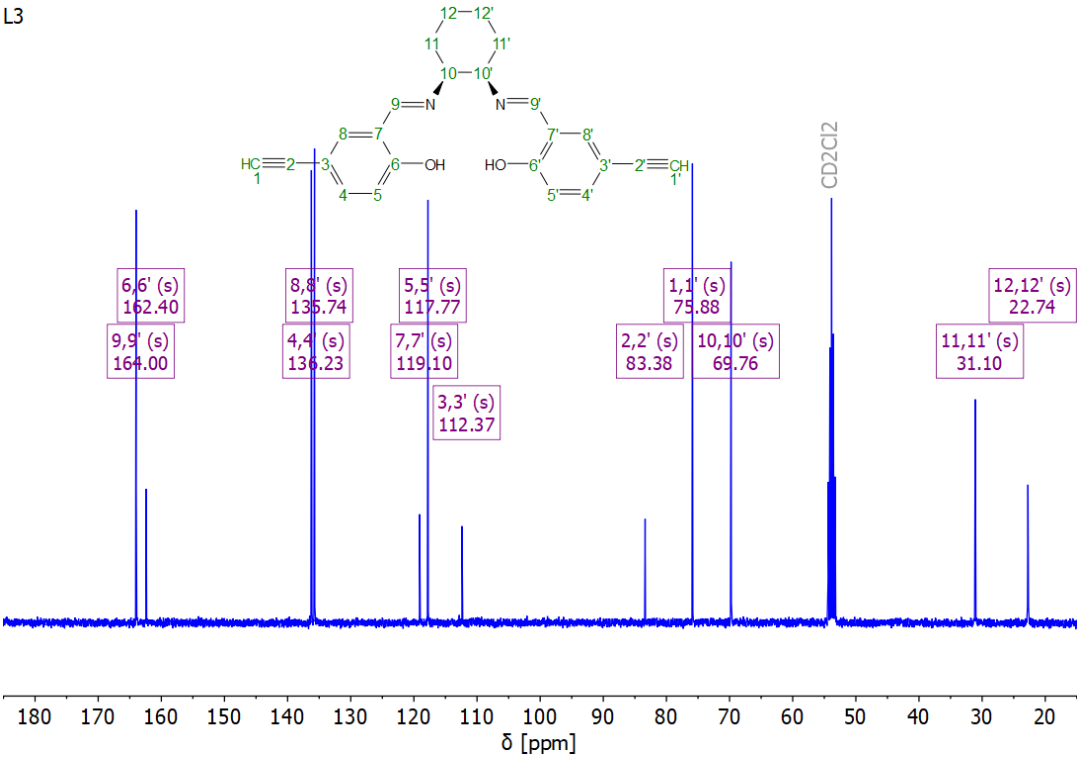

Figure S9: ^{13}C{^{1}H} NMR spectrum of **L3** ligand

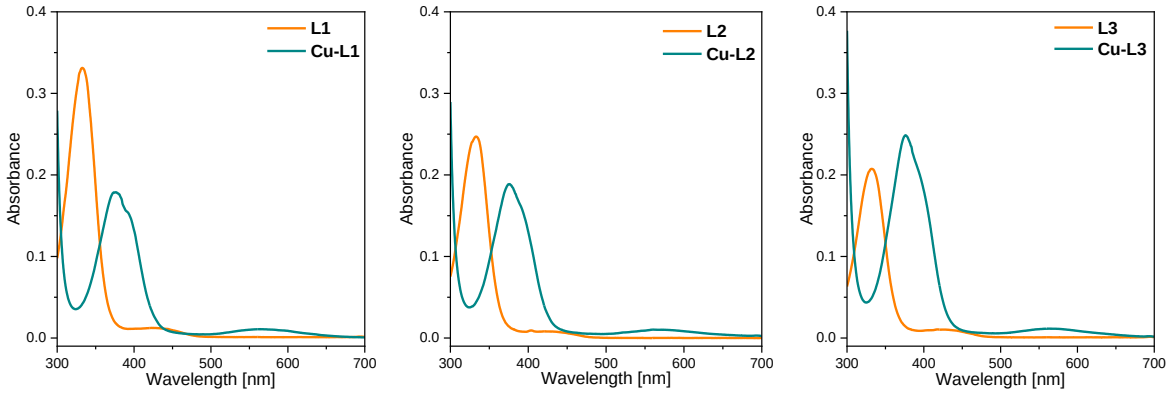

Figure S10: UV/VIS spectra of ligands (**L1**, **L2** and **L3**) and complexes (**Cu-L1**, **Cu-L2** and **Cu-L3**)

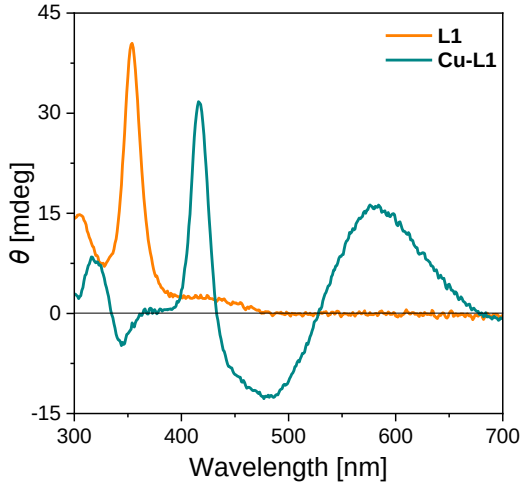

Figure S11: Circular dichroism (CD) spectra of ligand **L1** and complex **Cu-L1**.

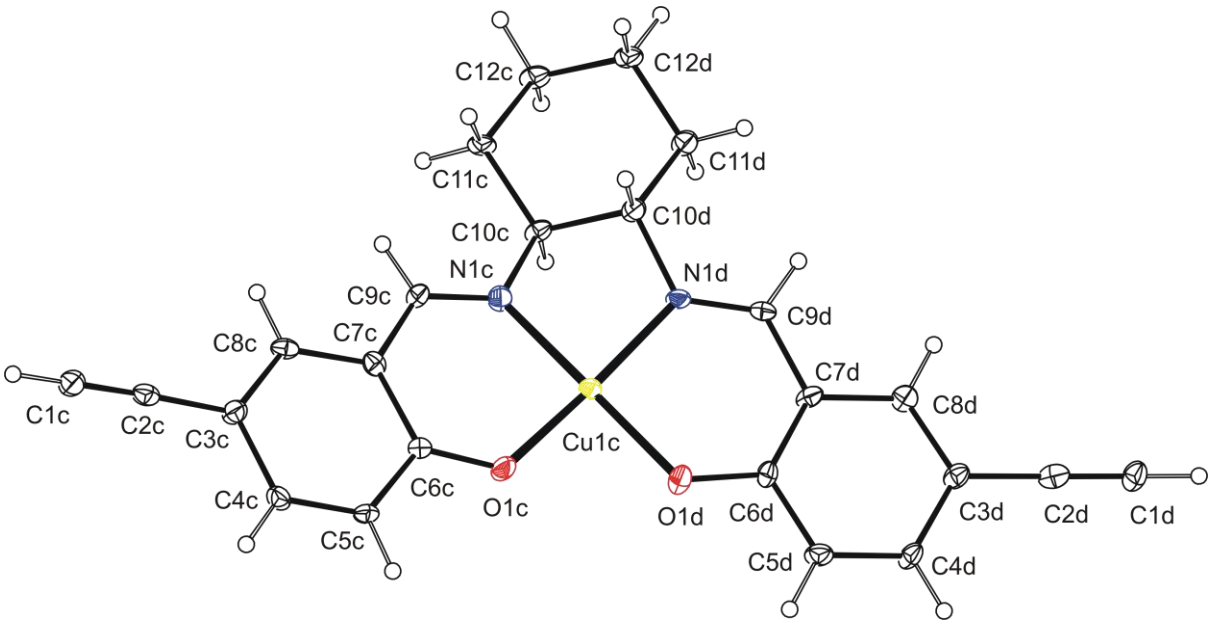

Figure S12: View on the one of two symmetrically independent molecule of **Cu-L1** with the atom numbering schema, the displacement ellipsoids are drawn at 50% probability level.

Crystal data for **Cu-L1**: $C_{24}H_{20}CuN_2O_2 \cdot C_3H_7NO$, M_r = 505.05; Monoclinic, $P2_1$, (No 4), a = 8.6380 (3) Å, b = 31.0524 (10) Å, c = 8.6749 (3) Å, β = 90.667 (2), V = 2326.72

(14) Å^3, Z = 4, D_x = 1.442 Mg m^{-3}, brown plate of dimensions 0.28 × 0.16 × 0.03 mm, multi-scan absorption correction (μ = 1.61 mm^{-1}) T_{min} = 0.79, T_{max} = 0.96; a total of 24115 measured reflections (θ_{max}= 68.4˚), from which 8359 were unique (R_{int} = 0.050) and 7893 observed according to the $I > 2\sigma(I)$ criterion. The refinement converged (Δ/σ_{max}= 0.001) to R = 0.061 for observed reflections and w$R(F^2)$ = 0.143, GOF = 1.16 for 617 parameters and all 8359 reflections. The final difference map displayed no peaks of chemical significance ($\Delta\rho_{max}$ = 0.60, $\Delta\rho_{min}$ -0.88 e.Å^{-3}).

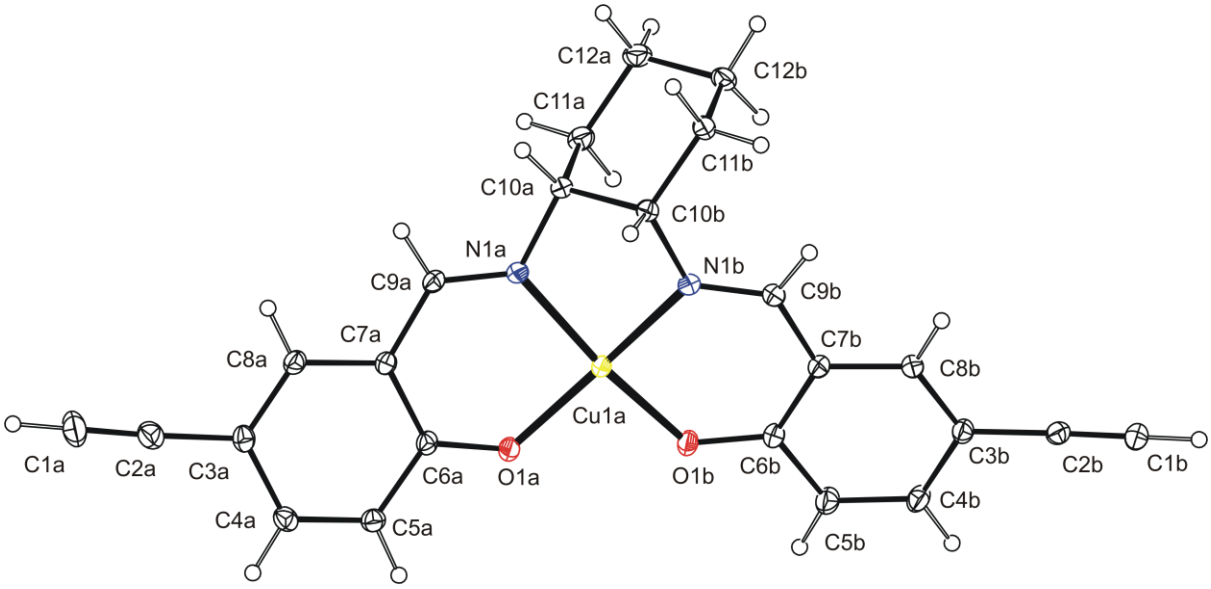

Figure S13: View on molecule of **Cu-L3** with the atom numbering schema, the displacement ellipsoids are drawn at 50% probability level.

Crystal data for **Cu-L3**: $C_{24}H_{20}CuN_2O_2$, M_r = 431.96; Monoclinic, $P2_1/n$, (No 14), a = 14.1633 (10) Å, b = 9.0797 (7) Å, c = 16.0469 (11) Å, β = 112.615 (2), V = 1904.9 (2) Å^3, Z = 4, D_x = 1.506 Mg m^{-3}, green prism of dimensions 0.25 × 0.10 × 0.07 mm, multi-scan absorption correction (μ = 1.81 mm^{-1}) T_{min} = 0.77, T_{max} = 0.89; a total of 57728 measured reflections (θ_{max}= 77.5˚), from which 4036 were unique (R_{int} = 0.031) and 3854 observed according to the $I > 2\sigma(I)$ criterion. The refinement converged (Δ/σ_{max}= 0.001) to R = 0.032 for observed reflections and w$R(F^2)$ = 0.088, GOF = 1.04 for 262 parameters and all 4036 reflections. The final difference map displayed no peaks of chemical significance ($\Delta\rho_{max}$ = 0.67, $\Delta\rho_{min}$ -0.70 e.Å^{-3}).

X-ray crystallographic data have been deposited with the Cambridge Crystallographic Data Centre (CCDC) under deposition number 2333975 and 2333976 for **Cu-L1** and **Cu-L3**, respectively and can be obtained free of charge from the Centre via its website (https://www.ccdc.cam.ac.uk/structures/).

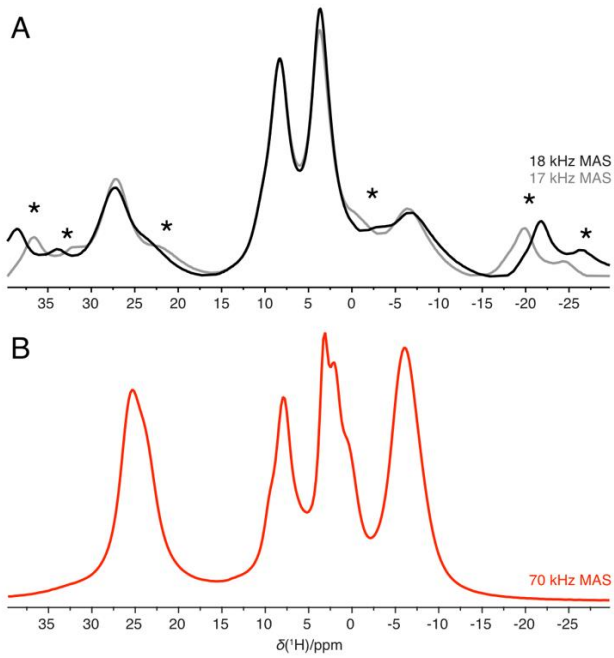

Figure S14: Comparison of slow and fast MAS ^{1}H NMR spectra of **Cu-L1**.

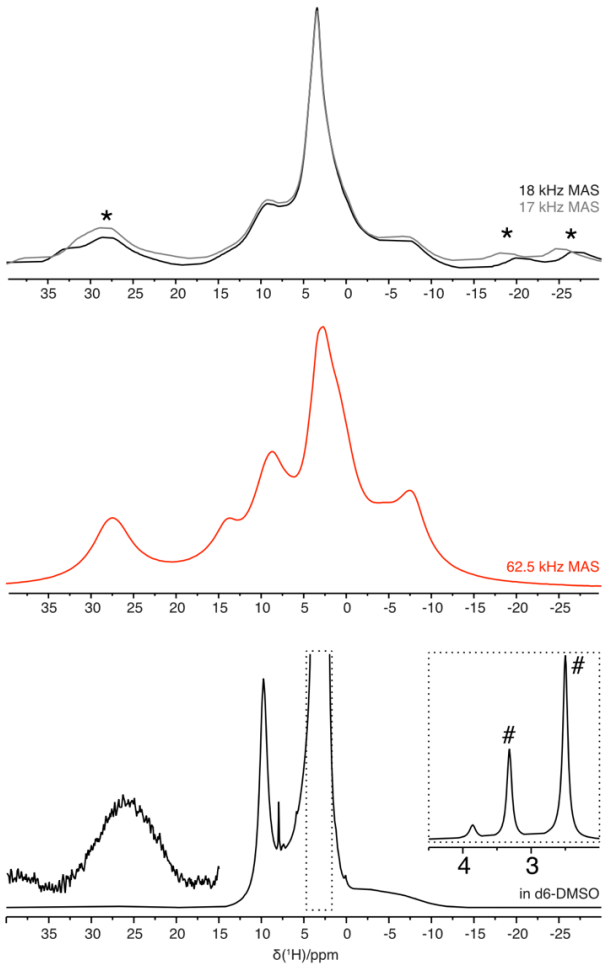

Figure S15: Comparison of slow and fast MAS ^{1}H NMR spectra of **Cu-L3** and solution ^{1}H NMR spectra of **Cu-L3**.

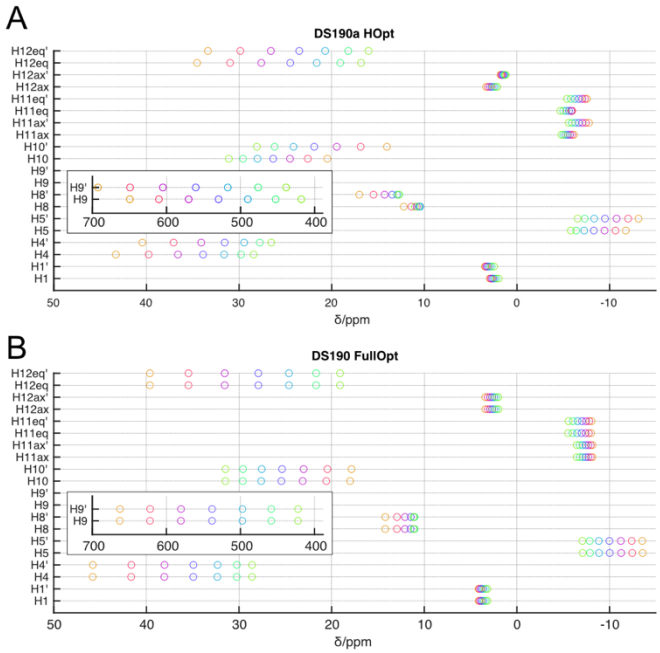

Figure S16: ^{1}H NMR shifts of **Cu-L1** predicted by calculations for X-ray based geometry with refined ^{1}H positions (A) and fully optimized geometry in COSMO/$CHCl_3$ solvent model (B) calculated for range of HFX admixture (from orange 10% for green 40% in 5% steps) (298 K).

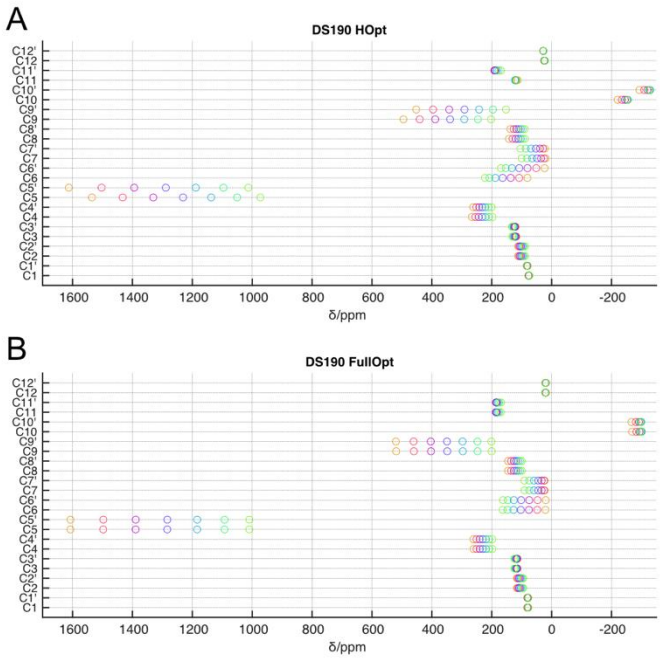

Figure S17: ^{13}C NMR shifts of **Cu-L1** predicted by calculations for X-ray based geometry with refined ^{1}H positions (A) and fully optimized geometry in COSMO/$CHCl_3$ solvent model (B) calculated for range of HFX admixture (from orange 10% for green 40% in 5% steps) (298 K).

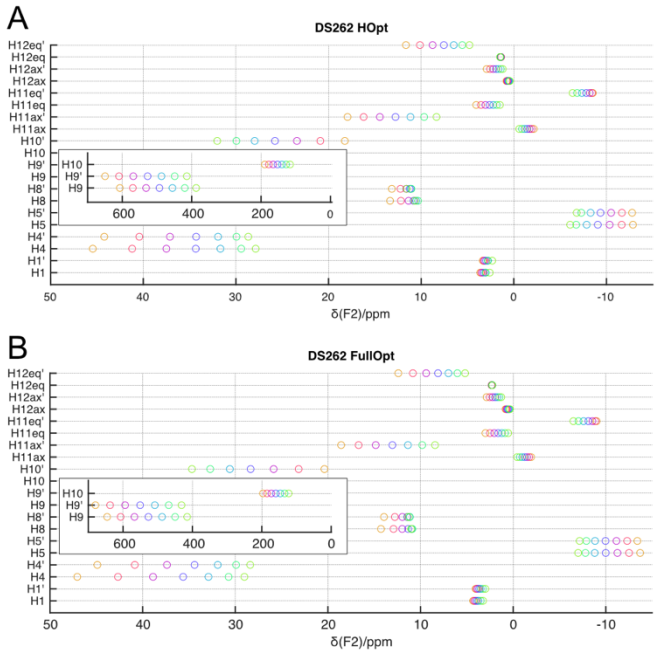

Figure S18: ^{1}H NMR shifts of **Cu-L3** predicted by calculations for X-ray based geometry with refined ^{1}H positions (A) and fully optimized geometry in COSMO/$CHCl_3$ solvent model (B) calculated for range of HFX admixture (from orange 10% for green 40% in 5% steps) (298 K).

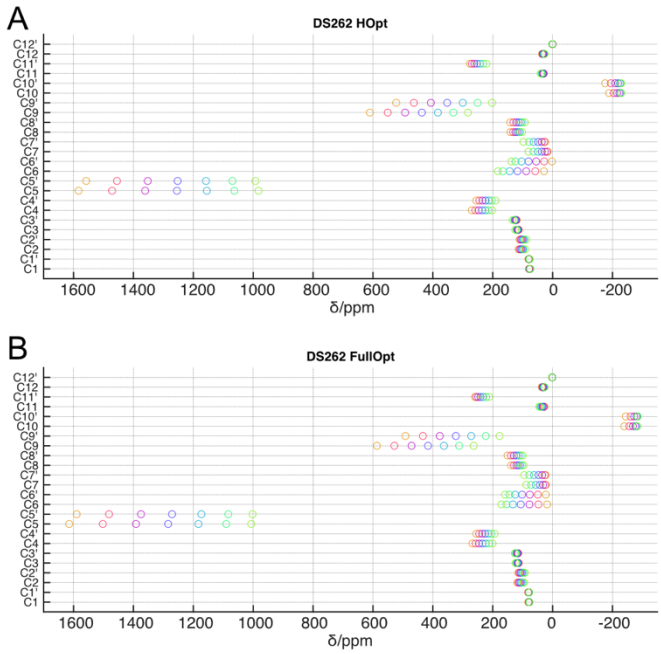

Figure S19: ^{13}C NMR shifts of **Cu-L3** predicted by calculations for X-ray based geometry with refined ^{1}H positions (A) and fully optimized geometry in COSMO/$CHCl_3$ solvent model (B) calculated for range of HFX admixture (from orange 10% for green 40% in 5% steps) (298 K).

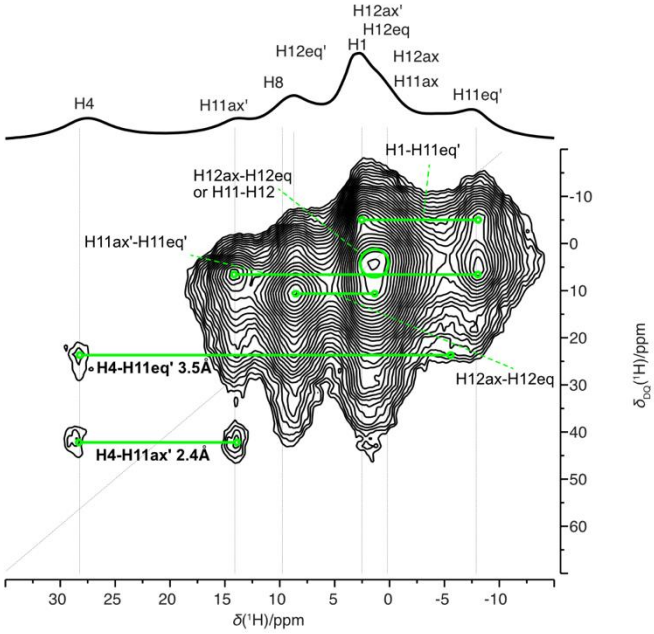

Figure S20: Homonuclear BaBa16 ^{1}H single-double quantum (SQ-DQ) correlation of **Cu-L3**.

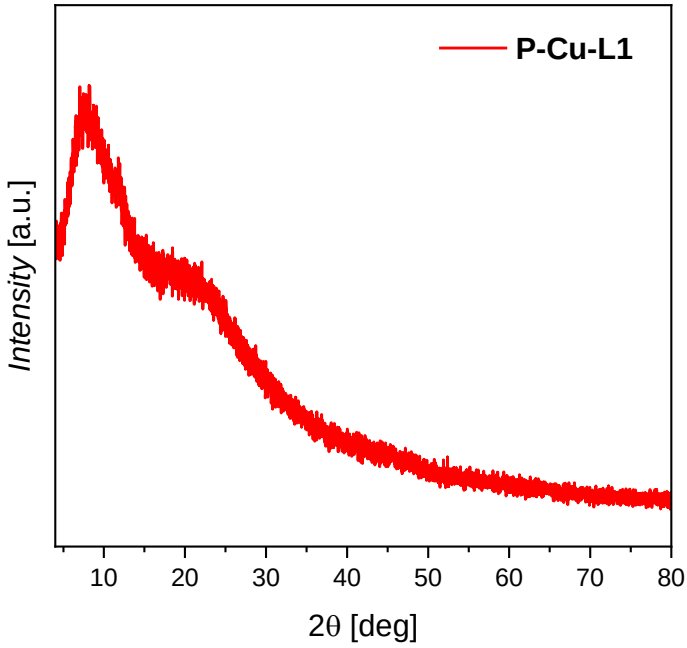

Figure S21: Powder X-Ray Diffraction (pXRD) pattern of network **P-Cu-L1**.

Powder X-ray Diffraction (XRD) pattern was collected using a high-resolution Explorer diffractometer (GNR Analytical Instruments, Italy) equipped with a one-dimensional Mythen 1K silicon strip detector (Dectris, Switzerland). A Cu X-Ray tube (wavelength λ = 1.54 Å) operated at 40 kV and 30 mA and monochromatized with Ni foil (β filter) was used. Measurements were performed in the 2θ range of 5 – 80° with a 0.1° step and 15 s exposure time at each step.

Table S1: Observed ^{1}H and ^{13}C NMR shift from HSQC-TEDOR experiment of **Cu-L1** a related calculated value for 10%, 25% and 40% of Hartee-Fock exchange admixture (at 298 K) and for various temperature 298 K and 323 K (using 25% HFX), as well as decomposition of calculated NMR shift (298 K, 25% HFX) to orbital shift ($\delta_{dia,K} = \sigma_{ref} - \sigma_{dia,K}$), Fermi contact ($\sigma_{FC}$) and spin-dipolar ($\sigma_{SD}$) shielding. All values listed in ppm, for atom label see Scheme 1.

	δ_{exp}	$\delta_{\mathrm{calc}}^{10\%}$	$\delta_{\mathrm{calc}}^{25\%}$	$\delta_{\mathrm{calc}}^{40\%}$	$\delta_{\mathrm{calc}}^{298\mathrm{K}}$	$\delta_{\mathrm{calc}}^{323\mathrm{K}}$	$\delta_{\mathrm{dia},K}$	σ_{FC}	σ_{SD}
H1	3.9	4.13	3.77	3.18	3.77	3.70	2.81	-1.01	0.05
H4	24.5	45.79	34.93	28.59	34.93	32.82	7.76	-27.36	0.20
H5	ND	-13.55	-10.00	-7.08	-10.00	-8.68	7.14	16.51	0.63
H8	8.9	14.21	11.47	11.15	11.47	11.16	7.54	-4.24	0.31
H9	ND	662.79	538.35	422.32	538.35	497.34	8.31	-530.81	0.77
H10	ND	17.93	25.39	31.47	25.39	23.67	3.14	-22.44	0.19
H11ax	-5.8	-8.16	-7.43	-6.45	-7.43	-6.76	1.24	8.34	0.32
H11eq	-5.8	-8.04	-7.00	-5.55	-7.00	-6.27	2.48	9.02	0.46
H12ax	1.6	3.42	2.66	2.00	2.66	2.56	1.36	-1.48	0.18
H12eq	25.0	39.63	27.91	19.09	27.91	25.91	2.02	-26.09	0.19
C1	80.4	81.5	78.8	77.8	78.8	79.0	82.08	3.14	0.17
C2	Q	115.9	105.9	94.4	105.9	104.7	90.16	-15.85	0.10
C3	Q	114.1	117.4	124.3	117.4	117.2	114.34	-3.44	0.38
C4	214	261.0	229.8	198.2	229.8	223.6	149.74	-81.55	1.52
C5	ND	1607.0	1283.6	1009.5	1283.6	1194.4	131.63	-1153.34	1.41
C6	Q	20.2	102.4	162.9	102.4	108.5	180.85	74.40	4.04
C7	Q	23.2	44.8	90.8	44.8	51.0	125.66	78.53	2.37
C8	99	145.7	118.4	99.9	118.4	120.9	150.85	31.31	1.12
C9	NA	519.6	349.0	200.9	349.0	335.3	170.89	-184.00	5.84
C10	NA	-267.7	-298.4	-296.2	-298.4	-269.7	71.59	367.18	2.77
C11	162	184.0	183.7	169.4	183.7	171.9	31.57	-153.36	1.27
C12	24	19.2	20.7	21.3	20.7	21.2	27.85	6.76	0.40

ND – not detected signal, Q - quaternary carbon

Table S2: Observed ^{1}H and ^{13}C NMR shift from HSQC-TEDOR experiment of **Cu-L3** a related calculated value for 10%, 25% and 40% of Hartee-Fock exchange admixture (at 298 K) and for various temperature 298 K and 323 K (using 25% HFX), as well as decomposition of calculated NMR shift (298 K, 25% HFX) to orbital shift ($\delta_{dia,K} = \sigma_{ref} - \sigma_{dia,K}$), Fermi contact ($\sigma_{FC}$) and spin-dipolar ($\sigma_{SD}$) shielding. All values listed in ppm, for atom label see Scheme 1.

Values in ppm:	δ_{exp}	$\delta_{\mathrm{calc}}^{10\%}$	$\delta_{\mathrm{calc}}^{25\%}$	$\delta_{\mathrm{calc}}^{40\%}$	$\delta_{\mathrm{calc}}^{298\mathrm{K}}$	$\delta_{\mathrm{calc}}^{323\mathrm{K}}$	$\delta_{\mathrm{dia},K}$	σ_{FC}	σ_{SD}
H1	2.7	4.32	3.90	3.26	3.90	3.82	2.81	-1.14	0.05
H1'	2.7	4.05	3.67	3.01	3.67	3.61	2.82	-0.90	0.05
H4	27.5	47.06	35.63	29.02	35.63	33.47	7.76	-28.06	0.19
H4'	28.5	44.89	34.39	28.39	34.39	32.33	7.77	-26.83	0.21
H5	ND	-13.70	-9.99	-7.01	-9.99	-8.67	7.13	16.50	0.62
H5'	ND	-13.41	-9.97	-7.17	-9.97	-8.64	7.15	16.46	0.65
H8	9.5	14.27	11.34	11.02	11.34	11.04	7.52	-4.12	0.30
H8'	9.5	13.95	11.44	11.36	11.44	11.14	7.55	-4.22	0.33
H9	ND	645.79	526.92	415.16	526.92	486.79	8.22	-519.47	0.76
H9'	ND	679.57	550.72	431.41	550.72	508.77	8.37	-543.14	0.79
H10	ND	196.70	159.64	122.54	159.64	147.53	3.15	-157.47	0.98
H10'	ND	20.38	28.35	34.68	28.35	26.45	3.84	-24.76	0.26
H11ax	-8.0	-1.93	-1.25	-0.43	-1.25	-0.99	2.08	4.48	-1.15
H11ax'	13.6	18.57	13.04	8.44	13.04	12.15	1.55	-11.91	0.42
H11eq	0.8	2.99	1.62	0.54	1.62	1.62	1.61	0.26	-0.26
H11eq'	0.8	-9.01	-8.11	-6.50	-8.11	-7.29	2.58	10.19	0.51
H12ax	0.8	0.83	0.57	0.35	0.57	0.63	1.36	0.67	0.12
H12ax'	1.1	2.88	1.94	1.29	1.94	1.89	1.30	-0.72	0.07
H12eq	0.8	2.34	2.29	2.26	2.29	2.25	1.82	-0.37	-0.09
H12eq'	8.5	12.40	8.12	5.19	8.12	7.60	1.41	-6.83	0.12
C1	85.3	81.2	78.5	77.7	78.5	78.8	82.2	3.5	0.2

C1'	85.3	81.9	79.4	78.9	79.4	79.6	82.2	2.7	0.2
C2	Q	117.7	107.2	95.2	107.2	105.9	90.1	-17.2	0.1
C2'	Q	114.7	104.7	92.6	104.7	103.5	90.1	-14.7	0.1
C3	Q	113.3	116.6	123.7	116.6	116.4	114.4	-2.6	0.4
C3'	Q	114.9	118.7	126.5	118.7	118.3	114.5	-4.5	0.4
C4	214	268.0	234.5	201.2	234.5	227.9	149.7	-86.3	1.5
C4'	202	255.3	225.0	193.7	225.0	219.2	149.9	-76.7	1.6
C5	ND	1614.5	1284.1	1006.8	1284.1	1194.9	131.6	-1153.8	1.3
C5'	ND	1589.5	1271.0	1002.2	1271.0	1182.9	131.6	-1140.9	1.5
C6	Q	18.2	106.4	171.3	106.4	112.2	181.2	71.0	3.8
C6'	Q	22.9	102.1	159.1	102.1	108.2	180.6	74.2	4.2
C7	Q	22.8	42.6	87.9	42.6	49.0	125.7	80.9	2.3
C7'	Q	23.1	47.2	95.0	47.2	53.2	125.8	76.3	2.4
C8	101	138.5	113.9	97.0	113.9	116.7	150.2	35.2	1.1
C8'	101	150.6	120.8	100.0	120.8	123.1	150.8	28.9	1.2
C9	ND	586.9	416.1	263.5	416.1	397.3	173.0	-248.7	5.6
C9'	ND	491.7	323.1	177.3	323.1	311.5	173.9	-155.3	6.1
C10	ND	-239.3	-276.5	-281.1	-276.5	-249.3	75.1	348.8	2.8
C10'	ND	-244.2	-279.8	-281.8	-279.8	-253.1	65.5	342.6	2.8
C11	33.1	27.4	34.6	44.5	34.6	34.7	35.6	1.3	-0.3
C11'	~240	259.3	241.0	211.8	241.0	224.4	26.5	-215.6	1.1
C12	33.1	36.3	31.1	26.6	31.1	30.9	27.9	-3.2	0.0
C12'	7.8	1.0	1.5	1.9	1.5	2.9	20.3	18.6	0.2

ND – not detected signal, Q - quaternary carbon

Table S3: Results achieved in repeating application of **P-Cu-L1** as heterogeneous catalyst of styrene oxidation.

	Styrene conversion [%]	Selectivity [%]	
		Styrene oxide	Benzaldehyde
1st cycle	80	41	40
2nd cycle	88	30	53
3rd cycle	96	18	51